Correspondence

Histogram of Oriented Lines for Palmprint Recognition

Wei Jia, *Member, IEEE,* Rong-Xiang Hu, Ying-Ke Lei, Yang Zhao, and Jie Gui

***Abstract*—Subspace learning methods are very sensitive to the illumination, translation, and rotation variances in image recognition. Thus, they have not obtained promising performance for palmprint recognition so far. In this paper, we propose a new descriptor of palmprint named histogram of oriented lines (HOL), which is a variant of histogram of oriented gradients (HOG). HOL is not very sensitive to changes of illumination, and has the robustness against small transformations because slight translations and rotations make small histogram value changes. Based on HOL, even some simple subspace learning methods can achieve high recognition rates.**

***Index Terms*—Biometric, histogram of oriented gradients (HOG), palm line, palmprint recognition, subspace learning.**

I. Introduction

In recent years, palmprint recognition has drawn wide attention from researchers. In general, palmprint recognition is using the palm of the person to identify or verify who the person is. Some previous researches have shown that, compared with fingerprint or iris-based personal biometrics systems, palmprint-based biometrics system has several special advantages, such as stable line features, less distortion, and easy self positioning. And, it can also obtain high-recognition rate with fast processing speed [1]. For the aforementioned reasons, nowadays the research related to palmprint recognition is becoming more and more active.

So far, there have been many approaches proposed for palmprint recognition [1]–[12]. Kong *et al.* [2] made a survey for these approaches and divided them into several different categories. For texture-based approaches, wavelet transform, discrete cosine transform, local binary pattern (LBP), and other statistical methods were used for texture feature extraction [2]. There are also some line-based approaches as lines including principal lines and wrinkles are essential and basic features of palmprint [3], [4]. It has been proved that coding-based approaches including ordinal code [5], robust line orientation code (RLOC) [6], competitive code [7], [8] and binary orientation co-occurrence vector [9] have achieved promising recognition performance. Recently, correlation methods such as optimal tradeoff synthetic discriminant function filter [10] and band-limited phase only correlation filter (BLPOC) [11] have also been successfully adopted for palmprint recognition.

In the past two decades, the study on subspace learning techniques was also very active [13]–[19]. Many different representative subspace learning methods have been proposed. In the early stage of the research in this field, almost all representative algorithms including principal component analysis (PCA) [13] and linear discriminant analysis (LDA) [13] require that the 2-D image data must be reshaped into 1-D vector, which can be referred to as the strategy of "image-as-vector." In recent years, some important progress has been made in the research of subspace learning. Among them, three strategies should be highlighted. The first strategy is the kernel method, which uses a linear classifier algorithm to solve nonlinear problems by mapping the original nonlinear observations into a higher dimensional space. Kernel PCA (KPCA) [14] and kernel LDA (KLDA) [14] are two representative kernel-based methods. The second strategy is the manifold learning method, which is based on the idea that the data points are actually samples from a low-dimensional manifold that is embedded in a high-dimensional space. The last strategy is matrix and tensor embedding methods. Matrix embedding methods, such as 2-D PCA (2DPCA) [15] and 2-D LDA (2DLDA) [16], can extract a feature matrix using a straightforward image projection technique. In addition, tensor embedding methods, such as tensor subspace analysis (TSA) [17], concurrent subspaces analysis (CSA) [18], and multilinear discriminant analysis (MDA) [19], can represent the image ensembles by a higher order tensor and extract low-dimensional features using multilinear algebra methods.

The subspace learning methods have been widely applied to biometrics including palmprint recognition. Lu *et al.* [20] and Wu *et al.* [21] proposed two methods based on PCA and LDA, respectively. Connie *et al*. [22] proposed several PCA/LDA/Independent component analysis-based approaches. Hu *et al*. [23] employed 2-D locality preserving projections (2DLPP), Yang *et al*. [24] proposed unsupervised discriminant projection, and Zuo *et al*. [25] presented a post-processed LDA for palmprint recognition. In general, these aforementioned approaches were directly applied to original palmprint images. In this paper, we call original image as original representation (OR) of palmprint. However, subspace learning methods utilizing OR have one obvious shortcoming, i.e., they are sensitive to illumination, translation, and rotation variances even if these variances are small. Thus, the recognition rates

Manuscript received December 12, 2011; revised February 10, 2013; accepted February 10, 2013. This work was supported in part by the National Science Foundation of China, under Grant 61175022, Grant 61100161, Grant 61272333, and Grant 60705007, and by grants from the Knowledge Innovation Program of the Chinese Academy of Sciences. This paper was recommended by Associate Editor M. Kamel.

W. Jia and R.-X. Hu are with the Institute of Nuclear Energy Safety Technology, Chinese Academy of Science, Hefei 230031, China (e-mail: icg.jiawei@gmail.com; hurongxiang2008@gmail.com).

Y.-K. Lei is with the Electronic Engineering Institute, Hefei, Anhui 230037, China (e-mail: leiyingke@gmail.com).

Y. Zhao is with the Department of Automation, University of Science and Technology of China, Hefei 230027, China (e-mail: zyknight@mail.ustc.edu.cn).

J. Gui is with the Institute of Intelligent Machines, Chinese Academy of Science, Hefei 230031, China (e-mail: guijiejie@gmail.com).

Color versions of one or more of the figures in this paper are available online at http://ieeexplore.ieee.org.

Digital Object Identifier 10.1109/TSMC.2013.2258010

of subspace learning methods are obviously worse than that of coding and correlation-based methods. In order to increase the discriminating power, Gabor wavelet representation (GWR) was often exploited to help impove the performance of subspace learning methods. Ekinci and Aykut [26] proposed a palmprint recognition approach integrating GWR and KPCA. Pan and Ruan [27], [28]. proposed two approaches using Gabor feature, in which $(2D)^2$PCA and 2DLPP were adopted for dimensionality reduction, respectively. However, the drawback of GWR is its high-computational cost. Although some researchers exploited Adaboost algorithm to select a sub-set of GWR to improve the computational efficiency and recognition performance, the effectiveness of this strategy has not been fully validated [29]. In [30], we proposed the directional representation (DR) of palmprint. Using DR, those subspace learning methods are robust to illumination variance. However, their sensitivity to translation and rotation variances has not been solved. From the above analysis, it can be seen that designing novel representation of palmprint, which is robust to slight illumination, translation, and rotation variances, is a crucial issue for subspace learning methods. Unfortunately, this issue has not been well discussed and solved until now.

Histogram of oriented gradients (HOG) descriptor was initially proposed by Lowe in his scale invariant feature transform (SIFT) [31]. Dalal and Trigges [32] proposed using HOG features to solve the pedestrian detection problem. Meanwhile, HOG descriptor has been successfully applied to other object detection and recognition tasks [33]. However, for palmprint recognition, gradient exploited in HOG is not a good tool to detect the line responses and orientation of pixels because different palm lines have different widths and there are complicated intersections between lines. In this paper, we propose the histogram of oriented lines (HOL) descriptor, a variant of HOG, for palmprint recognition, which exploits line-shape filters or tools such as the real part of Gabor filter and modified finite radon transform (MFRAT) [3] to extract line responses and orientation of pixels. Compared with OR, DR, and GWR, HOL has two obvious advantages. First, using oriented lines and histogram normalization, HOL has better invariance to changes of illumination. Second, HOL has the robustness against transformations because slight translations and rotations make small histogram value changes. In addition, line-shape filters and tools used in HOL can well calculate the line response and orientation of pixels. There is no doubt that, owing to these merits, HOL descriptor will help subspace learning methods achieve promising recognition rates.

II. HOL Descriptor

A. Brief Review of HOG

An example of generating HOG is depicted in Fig. 1.

Given an image I, the main steps of generating HOG are presented as follows:

Step 1: Divide the whole image into $n \times n$ non overlapping *Cells*. Each *Cell* contains $c_1 \times c_2$ pixels.

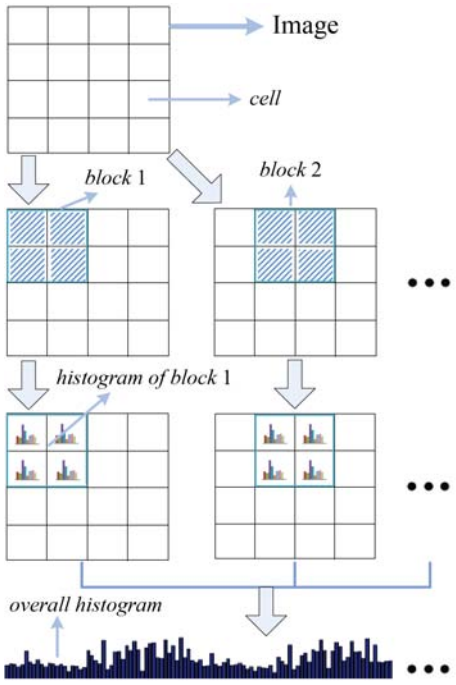

Fig. 1. Procedure of generating HOG.

Step 2: Construct a *Block* by integrating $b_1 \times b_2$ *Cell*s. Two adjacent *Blocks* can overlap.

Step 3: For each pixel, $I(x, y)$, the gradient magnitude $m(x, y)$, and orientation $\theta(x, y)$ are computed by

$$dx = I(x+1, y) - I(x-1, y) \tag{1}$$

$$dy = I(x, y+1) - I(x, y-1) \tag{2}$$

$$m(x, y) = \sqrt{dx^2 + dy^2} \tag{3}$$

$$\theta(x, y) = \tan^{-1}\left(\frac{dy}{dx}\right). \tag{4}$$

Step 4: Divide the orientation range (0°–180°) into k bins. And then calculate the histogram within *Cell* (HC)

$$\mathrm{HC}(k)_i = \mathrm{HC}(k)_i + m(x, y) \text{ if } I(x, y) \in Cell_i \text{ and } \theta(x, y) \in \mathrm{bin}(k)$$

Step 5: The histogram of a *Block* (HB) can be obtained by integrating the HCs within this *Block*

$$\mathrm{HB}_j = \{\mathrm{HC}_1, \mathrm{HC}_2, \ldots, \mathrm{HC}_{b_1 \times b_2}\}.$$

Then, normalize the vector of HB_j $(\mathrm{NHB})_j$ by *L2*-norm block normalization

$$\mathrm{NHB}_j = \frac{\mathrm{HB}_j}{\sqrt{\left\|\mathrm{HB}_j\right\|_2^2 + e^2}} \tag{5}$$

where e is a small constant to avoid the problem of division by zero. If there are N *Blocks* in an image, the last histogram, HOG, can be obtained by integrating all normalized *Block*'s histograms

$$\mathrm{HOG} = \left\{\mathrm{NHB}_1, \mathrm{NHB}_2, \ldots, \mathrm{NHB}_j, \ldots, \mathrm{NHB}_N\right\}. \tag{6}$$

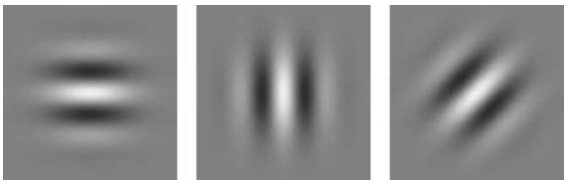

Fig. 2. Real parts of three Gabor filters at the angles of 0°, 90°, and 45°.

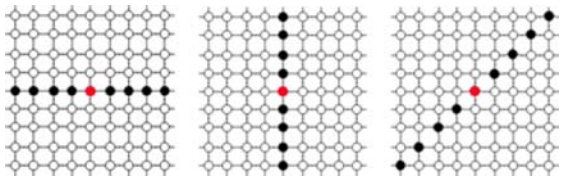

Fig. 3. 9×9 MFRAT at the angle of 0°, 90°, and 45°. Red point is the center of the lattice. Black and red points make up lines at different directions.

Generally, a *Block* consists of 2×2 *Cell*s.

B. HOL Descriptor

There are different line-shape filters or tools to extract line and orientation feature of a palmprint, e.g., the real part of Gabor filter used in competitive code [7], Gaussian filter adopted in ordinal code [5], and MFRAT utilized in RLOC [6]. In this paper, the real part of Gabor filter and MFRAT will be exploited to generate HOL descriptor of palmprint.

Gabor filter is a powerful tool in computer vision and pattern recognition. Recently, some new methods combining Gabor feature and local descriptors, such as local Gabor XOR patterns (LGXP) [34] and local Gabor binary patterns (LGBP) [35], have been proposed for face recognition and achieved impressive recognition performance.

In general, 2-D circular Gabor filter has the following form:

$$G(x, y, \theta, \mu, \sigma) = \frac{1}{2\pi\sigma^2}\exp\left\{-\frac{x^2+y^2}{2\sigma^2}\right\} \exp\{2\pi i(\mu x\cos\theta + \mu y\sin\theta)\} \quad (7)$$

where $i = \sqrt{-1}$, μ is the frequency of the sinusoidal wave, θ controls the orientation of the function, and σ is the standard deviation of the Gaussian envelop. Based on this Gabor function, a Gabor filter bank with one scale and k directions can be created. The direction θ_m is calculated as follows:

$$\theta_m = \frac{\pi(m-1)}{k}, \quad m = 1, 2, \ldots, k. \quad (8)$$

Three examples of the real part of Gabor filter at the angles of 0°, 90°, and 45°, are presented in Fig. 2.

Given a palmprint image I, the steps of extracting the line responses and orientation of pixels in palmprint using the real part of Gabor filter bank can be briefly summarized as follows.

Step 1: Convoluting image I using the real part of designed Gabor filter bank to generate M filtered images.

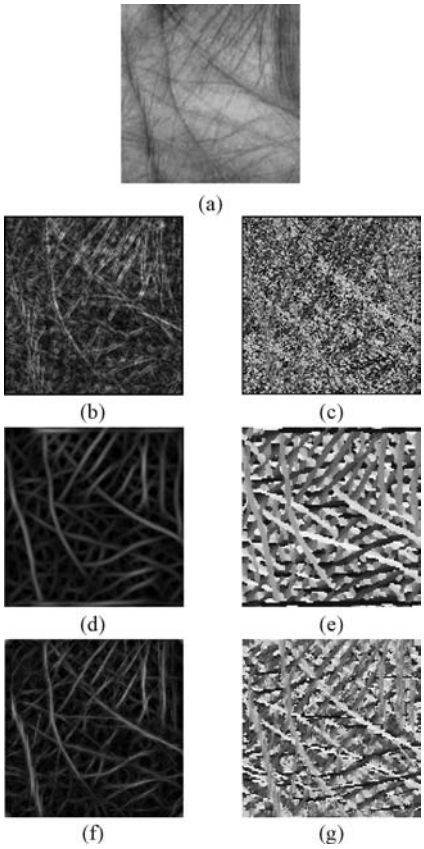

Fig. 4. Line response maps and orientation maps calculated by gradient, Gabor filter, and MFRAT. (a) Original palmprint image. (b) Line response map calculated by gradient. (c) Orientation map calculated by gradient. (d) Line response map calculated by Gabor filter. (e) Orientation map calculated by Gabor filter. (f) Line response map calculated by MFRAT. (g) Orientation map calculate by MFRAT.

Step 2: The response $m(x, y)_{\text{Gabor}}$ and orientation $\theta(x, y)_{\text{Gabor}}$ of each pixel can be obtained by the following two equations:

$$m(x, y)_{\text{Gabor}} = \min(I(x, y) * G(x, y, \theta_k)) \quad (9)$$

$$\theta(x, y)_{\text{Gabor}} = \arg\min_k(I(x, y) * G(x, y, \theta_k)) \quad (10)$$

where * means the convolution operation.

If we use $m(x, y)_{\text{Gabor}}$ and $\theta(x, y)_{\text{Gabor}}$ to replace $m(x, y)$ and $\theta(x, y)$ in (3) and (4), the HOL descriptor will be created. In this paper, the HOL descriptor created by Gabor filter is denoted as $\text{HOL}_{\text{Gabor}}$.

The MFRAT is defined as follows: denoting $Z_p = \{0, 1, \ldots, (p-1)\}$, where p is a positive integer, the MFRAT on the finite grid Z_p^2 is defined as

$$r[L_k] = \text{MFRAT}_f(k) = \sum_{i,j \in L_k} f[i, j] \quad (11)$$

where $f[x, y]$ is the pixel value located in (x, y) and L_k denotes the set of points that make up a line on the lattice Z_p^2, which means

$$L_k = \{(i, j) : j = S_k(i - i_0) + j_0, i \in Z_p\} \quad (12)$$

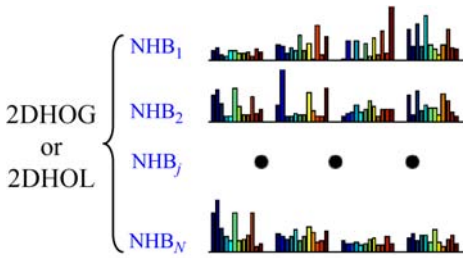

Fig. 5. 2DHOG or 2DHOL.

where (i_0, j_0) denotes the center point of the lattice Z_p^2 and k means the index value corresponding to a slope of S_k. That is to say, different k denotes different slopes of L_k. For any given k, the summation $r[L_k]$ of only one line, which passes through the center point (i_0, j_0) of Z_p^2, is calculated. Actually, $r[L_k]$ is the energy of line L_k.

In the MFRAT, if there is a genuine line which passes through the center point of Z_p^2, we can obtain the energy $m(x, y)_{\mathrm{MFRAT}}$ and orientation $\theta(x, y)_{\mathrm{MFRAT}}$ of this center point by the following equations:

$$m(x, y)_{\mathrm{MFRAT}} = \min(r[L_k]) \tag{13}$$

$$\theta(x, y)_{\mathrm{MFRAT}} = \arg\min_k(r[L_k]). \tag{14}$$

An example of MFRAT is depicted in Fig. 3. Similarly, if we use $m(x, y)_{\mathrm{MFRAT}}$ and $\theta(x, y)_{\mathrm{MFRAT}}$ to replace $m(x, y)$ and $\theta(x, y)$ in (3) and (4), the HOL descriptor will be created. Similarly, the HOL descriptor generated by MFRAT is denoted as $\mathrm{HOL}_{\mathrm{Radon}}$ in this paper.

Fig. 4 shows line response and orientation maps calculated by gradient, Gabor filter, and MFRAT. It should be noted that, in orientation map, different gray values denote different orientations. From Fig. 4, it can be seen that the real part of Gabor filter and MFRAT can better extract the line response map and orientation of pixels.

In (6), HOG is constructed as a vector. In fact, HOG or HOL can be created as a matrix as shown in Fig. 5, in which each row is NHB_j. For convenience, we call HOG or HOL in matrix form as 2DHOG or 2DHOL. Using 2DHOG and 2DHOL, some matrix or tensor-based subspace learning methods, such as 2DPCA [15], 2DLDA [16], TSA [17], CSA [18], and MDA [19], can be performed for dimensionality reduction.

III. Experiments

A. Databases

The proposed approach was tested on two palmprint databases, which are The Hong Kong Polytechnic University Palmprint Database II (PolyU II) [1] and the blue band of The Hong Kong Polytechnic University Multispectral Palmprint Database (PolyU M_B) [36].

PolyU II database contains 7752 grayscale palmprint images from 386 palms corresponding to 193 individuals. In this database, about 20 samples from each of these palms were collected in two sessions, where about 10 samples were captured in the first session and the remaining 10 samples were captured the second session. The total numbers of images captured in the first session and the second session are 3889 and 3863, respectively.

PolyU M_B database contains 6000 grayscale palmprint images from 500 palms corresponding to 250 individuals [36]. In this database, about 12 samples from each of these palms were collected in two sessions, where 6 samples were captured in the first session and the remaining 6 samples were captured in the second session.

In PolyU II database and PolyU M_B database, palmprint is orientated and the ROI image, whose size is 128×128, is cropped using the similar preprocessing approach described in the literature [1].

In this paper, we exploit several representative subspace learning methods for dimensionality reduction. For HOG and HOL, PCA, LDA, SRDA [37], and their kernel versions (KPCA, KLDA, and KSRDA) are exploited. For 2DHOG and 2DHOL, the methods of 2DPCA, 2DLDA, TSA, CSA, and MDA are used.

In our method, Euclidean distance is adopted for matching. A matching is conducted by the following steps.

Step 1: Extracting HOL descriptor from each image in training set and test set.

Step 2: Based on HOL descriptor, using subspace learing method for dimensionality reduction to get feature vectors (or matrices or tensors).

Step 3: The distance between two arbitrary feature vectors, $A = [a_1, a_2, \ldots, a_i]$ and $B = [b_1, b_2, \ldots, b_i]$, is defined by

$$d(A, B) = \sum_{j=1}^{i} \left\| a_j - b_j \right\|_2 \tag{15}$$

where $||a_j - b_j||_2$ denotes the Euclidean distance between two vectors.

In two databases, both verification and identification experiments are conducted.

Verification is a one-to-one comparison, which answers the question of 'whether the person is whom he claims to be.' In the verification experiments, the statistical value of equal error rate (EER) is adopted to evaluate the performance of different methods. In experiments, the statistical pairs of false reject rate (FRR) and false accept rate (FAR) were used to calculate EER. In a palmprint database, two image sets were constructed, i.e., training set and test set. Here, we suppose that each palm provides n palmprint training images (templates) in training set. To obtain the statistical pairs of FRR and FAR, each of the test images was matched with all of the templates in the training set. If the test image and the template are from the same palm, the matching between them is remarked as a correct matching. Likewise, an incorrect matching can also be defined in a similar manner. Because each palm has n templates in the training database, each test image can thus generate n scores. The maximum of them is regarded as a correct matching score at last. Similarly, when a test image matches with another template that comes from a different palm, n incorrect scores can be calculated, and the maximum of them is regarded as an incorrect verification matching score.

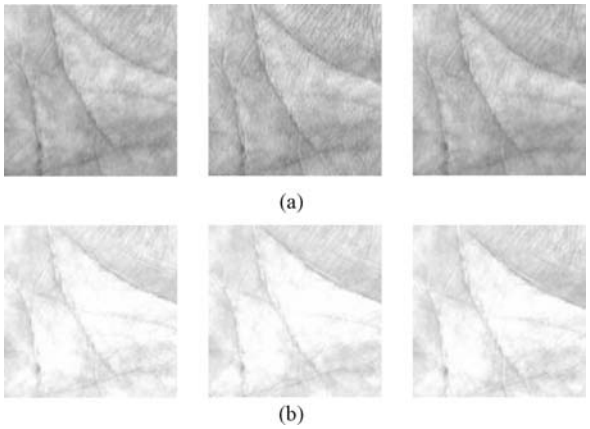

Fig. 6. Six palmprint ROI images from a same palm in PolyU II database. (a) Three images captured in the first session. (b) Three images captured in the second session.

After all test images matched with all templates in training set, the statistical values of FRR, FAR, and EER can be calculated.

Identification is a one-to-many comparison, which answers the question of who the person is. In this paper, the close-set identification is conducted. That is we know all enrollments exist in the training set. In order to obtain identification accuracy, the rank 1 identification rate (recognition rate) is used, in which a test image will be matched with all templates in training set, and the label of the most similar template will be assigned to this test image.

B. Experimental Results on PolyU II Database

Fig. 6 depicts six palmprint ROI images of PolyU II database, which were captured from a same palm but in different sessions. The three images in the first row [Fig. 6(a)] were captured in the first session while the images in the second row [Fig. 6(b)] were captured in the second session. It can be seen that there are drastic changes of illumination between the images captured in different sessions. In this regard, PolyU II is a challenging database. Before the experiments of HOG and HOL are conducted, some important parameters should be firstly determined such as the size of *Cell*, the number of direction bins k, the value of p in MFRAT, and the value of μ in Gabor filter. In PolyU II database, we use the first three palmprint images from the first session for training (1158 images) and use the remaining palmprint images (2731 images) from the first session as the validation set to determine parameters. All palmprint images (3863 images) from the second session are used as probe images to evaluate the recognition performance of the proposed method.

For HOG and HOL, after conducting numerous experiments using validation set, the size of a *Cell* is determined as 16×16, and the number of bins k is determined as 12. As a result, for a palmprint ROI image with the size of 128×128, there are total 64 (8×8) *Cell*s and 49 (7×7) *Block*s, and the dimension of overall histogram is 2352 ($12 \times 2 \times 2 \times 49$). Consequently, the size of 2DHOG and 2DHOL is 49×48.

For $\text{HOL}_{\text{Gabor}}$, the value of σ in Gabor filter is set to 5.6179 [1]. Thus, the only parameter of Gabor filter we will determine is μ, which controls the band width of Gabor filter.

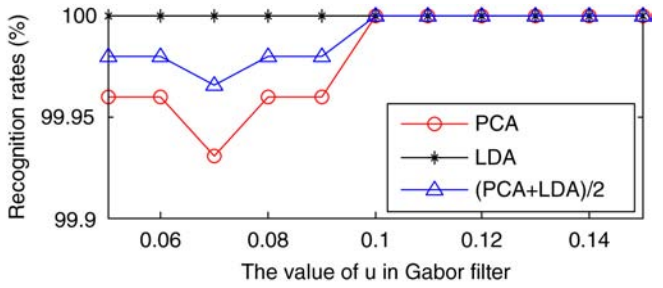

Fig. 7. Recognition rates of PCA, LDA, and (PCA + LDA)/2 on $\text{HOL}_{\text{Gabor}}$ descriptor under different values of μ in Gabor filter.

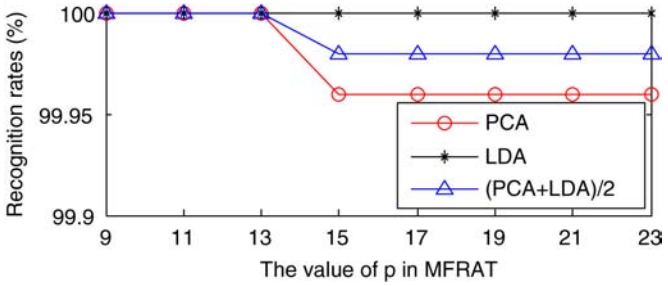

Fig. 8. Recognition rates of PCA, LDA, and (PCA + LDA)/2 on $\text{HOL}_{\text{Radon}}$ descriptor under different values of p in MFRAT.

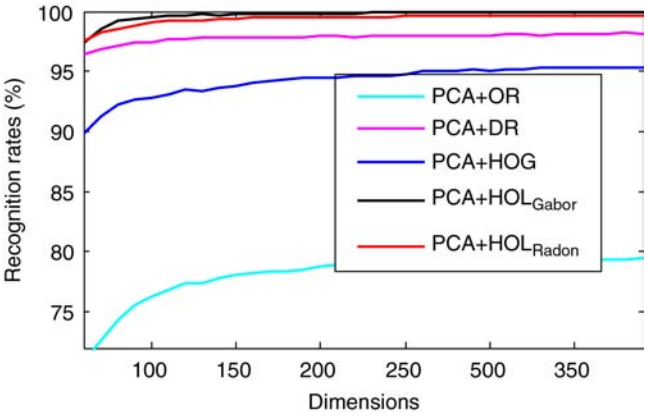

Fig. 9. Recognition rates of PCA on different representations.

For $\text{HOL}_{\text{Radon}}$, the only parameter is the value of p in MFRAT. Two experiments are conducted on validation set for parameter selection. And the mean of recognition rates of PCA and LDA, which is denoted as (PCA + LDA)/2, is exploited as the evaluation criterion. Fig. 7 depicts the recognition rates of PCA, LDA, and (PCA + LDA)/2 on $\text{HOL}_{\text{Gabor}}$, while the value of μ changes from 0.04 to 0.16 at the interval of 0.01. It can be seen that the (PCA + LDA)/2 achieves recognition rate of 100% when the value of μ is in the range of [0.1, 0.15]. In this paper, the value of μ in Gabor filter is selected as 0.11 in the remaining experiments. Fig. 8 depicts the recognition performance of (PCA + LDA)/2 on $\text{HOL}_{\text{Radon}}$. It can be seen that when the value of p in MFRAT is 9, 11, or 13, (PCA + LDA)/2 achieves recognition rate of 100%. Here, the value of p is selected as 11 in the remaining experiments.

We then conduct identification experiments using probe set. Figs. 9–11 depict the recognition rates of PCA, LDA, and

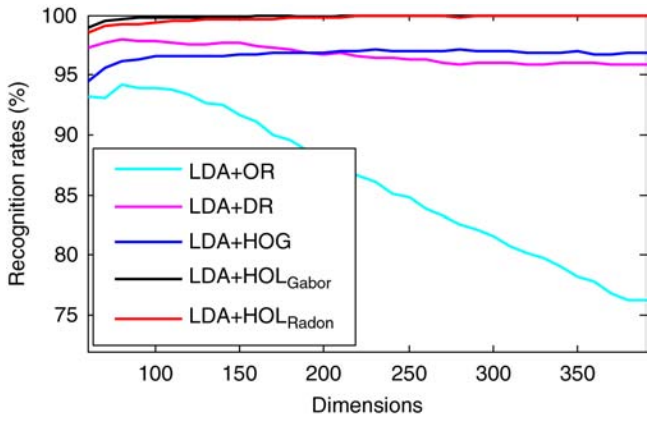

Fig. 10. Recognition rates of LDA on different representations.

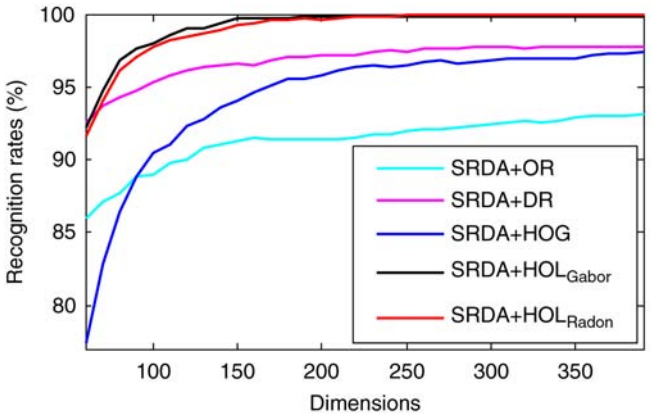

Fig. 11. Recognition rates of SRDA on different representations.

SRDA on different representations under different dimensions. Table I also lists the recognition rates and corresponding dimensions of vector-based subspace learning methods on different representations. From Figs. 9–11 and Table I, we can see that using $\text{HOL}_{\text{Gabor}}$ and $\text{HOL}_{\text{Radon}}$, all vector-based subspace learning methods achieved very high recognition rates. Particularly, the recognition rate of proposed method is 99.97%, which is a very promising recognition performance. Table II lists the recognition rates and corresponding dimensions of matrix or tensor-based subspace learning methods. From the experimental results, it can be concluded that the proposed HOL/2DHOL descriptors have more discriminative power than OR, DR, and HOG/2DHOG representations.

In Tables I and II, the recognition rates of several 'image-as-vector' methods, kernel-based methods, matrix and tensor-based methods are reported. The experimental results demonstrate that HOL or 2DHOL descriptor is valid for these representative subspace learning methods.

In Table III, we make a performance comparison of identification experiments between the proposed method and other methods, all of which were tested on PolyU II database. Here, we select the recognition rate (99.97%) of $\text{KSRDA} + \text{HOL}_{\text{Radon}}$ for performance comparison because it is the highest recognition rate achieved by the proposed method. The recognition rate of KPCA + GWR method proposed by Ekinci and Aykut is 95.17% reported in [26], which is much worse than that of the proposed method. It should be noted about 10 images of each palm captured in the first session are used for training in Ekinci's method. In this paper, we also conduct an experiment combining MDA and GWR. To do this, we use 40 Gabor wavelet kernels at the eight orientations and five scales to convolute a palmprint image to generate a third-order tensor, and then the MDA method is adopted for dimensionality reduction. The recognition rate of MDA + GWR method is 98.81% (the corresponding dimension is $9 \times 9 \times 7$), which is also obviously worse than that of the proposed method. These comparisons demonstrate that the proposed HOL is more discriminative than GWR. The recognition rate of post-processed LDA + OR method proposed recently is 96.97% [25]. This result again demonstrates that using OR, subspace learning methods cannot obtain desired recognition performance.

Using the experimental protocol same to the proposed method, we conduct the identification experiments of other methods, i.e., RLOC [6], original competitive code [7], ordinal code, BLPOC, LBP [34], LGXP [35], and LGBP [34] by ourselves. The recognition rates of them are listed in Table III. For LBP, LGXP, and LGBP methods, we adopted the parameters in their original literatures. In competitive code [7], two parameters of 2-D ellipsoidal Gabor filter ω and δ, were set to 0.5 and 1.5, respectively. In ordinal code [5], two parameters of 2-D Gaussian filter δ_x and δ_y, were set to 5 and 1, respectively. Meanwhile, the size of 2-D ellipsoidal Gabor filter in competitive code and 2-D Gaussian filter in ordinal code is 40×40. In RLOC [6], we use 16×16 MFRAT, whose width of the lines is four pixels, to extract RLOC feature. In BLPOC [11], because the ROI image of palmprint is a square and its Fourier spectrum is a square, the selected center area of the 2-D discrete Fourier transform spectrum is also a square, whose band size is $J \times J$. In the experiments on PolyU II database, the value of J is set to 32. It should be noted that peak-to-sidelobe ratio is adopted as similarity measure in BLPOC [38]. In the methods of LBP, LGXP, and LGBP, we use the same setting in [34], [35].

In Table III, it can be seen that the recognition rate of the proposed method is very close to the recognition rates of three orientation coding methods, i.e., RLOC, competitive code, and ordinal code, meanwhile, obviously better than that of methods of BLPOC, LBP, LGXP, and LGBP. It should be noted that the results of methods competitive code, ordinal code, BLPOC, LBP, LGXP, and LGBP are based on our reimplementation. Thus, bias may be unavoidable.

The results listed in Tables I and II demonstrate that the proposed HOL descriptor is valid for these representative subspace learning methods and has more discriminative power than OR, DR, and HOG/2DHOG representations. In addition, the results listed in Table III show that the performance of the proposed method is comparable to some leading palmprint recognition methods for identification. In other words, the results listed in Tables I–III demonstrate that the effectiveness of the proposed method from different aspects.

In verification experiments, five methods are tested, which are BLPOC, RLOC, ordinal code, competitive code, and the proposed method. Here, it should be noted that BLPOC,

TABLE I

RECOGNITION RATE (%) OF VECTOR-BASED METHODS ON DIFFERENT REPRESENTATIONS AND CORRESPONDING DIMENSION (IN THE INDENTIFICATION EXPERIMETS ON POLYU II DATABASE)

	PCA	KPCA	LDA	KLDA	SRDA	KSRDA
OR	79.42 (380)	79.42 (380)	94.15 (70)	94.72 (310)	93.09 (380)	94.77 (360)
DR	98.19 (370)	98.16 (380)	97.93 (70)	97.59 (360)	97.77 (290)	97.75 (340)
HOG	95.37 (360)	95.37 (350)	97.13 (220)	97.57 (380)	97.39 (380)	98.03 (360)
HOL_{Gabor}	99.87 (220)	99.84 (210)	99.92 (330)	99.95 (270)	99.84 (280)	99.95 (320)
HOL_{Radon}	99.69 (310)	99.69 (270)	99.95 (380)	99.95 (270)	99.97 (340)	99.97 (340)

TABLE II

RECOGNITION RATES (%) OF MATRIX OR TENSOR-BASED METHODS ON DIFFERENT REPRESENTATIONS AND CORRESPONDING DIMENSION (IN THE INDENTIFICATION EXPERIMETS ON POLYU II DATABASE)

	2DPCA	2DLDA	TSA	CSA	MDA
OR	80.43 (128×18)	95.11 (128×12)	95.05 (19×19)	96.45 (10×10)	96.92 (11×11)
DR	98.63 (128×17)	99.07 (128×15)	99.15 (15×15)	98.73 (12×12)	99.33 (13×13)
2DHOG	95.68 (49×35)	96.19 (49×26)	95.99 (40×40)	92.83 (31×31)	94.33 (23×23)
$2DHOL_{Gabor}$	99.84 (49×32)	99.90 (49×19)	99.90 (35×35)	99.90 (34×34)	99.87 (29×29)
$2DHOL_{Radon}$	99.66 (49×29)	99.77 (49×28)	99.77 (39×39)	99.82 (20×20)	99.84 (34×34)

TABLE III

RECOGNITION RATE OF DIFFERENT METHODS IN IDENTIFICATION EXPERIMENTS

Method	Recognition rate (%)
KPCA + GWR [26]	95.17
Post-processed LDA + OR [25]	96.97
MDA + GWR	98.81
RLOC	100
Competitive code	100
Ordinal code	100
BLPOC	99.53
LBP	82.32
LGXP	99.51
LGBP_Phase	99.56
LGBP_Magtitude	99.28
Proposed method	99.97

TABLE IV

EER OF DIFFERENT METHODS IN VERIFICATION EXPERIMENTS CONDUCTED ON POLYU II DATABASE

	EER(%)
BLPOC	0.24
RLOC	0.057
Ordinal code	0.025
Competitive code	0.048
Proposed method	0.31

RLOC, ordinal code, and competitive code are four representative methods for palmprint recognition. Among all kinds of the proposed methods, we select $LDA + HOL_{Radon}$ to conduct verification experiment. Here, the dimension of LDA is set to 380. The EERs of these methods are listed in Table IV. In order to better illustrate the verification performances, the receiver operating characteristic (ROC) curves of five methods are illustrated in Fig. 12, which plots the FAR against the genuine accept rate (GAR). From Table IV and Fig. 12, it can be seen that the verification performance of the proposed method is near to BLPOC, but far worse than that of three orientation-based methods.

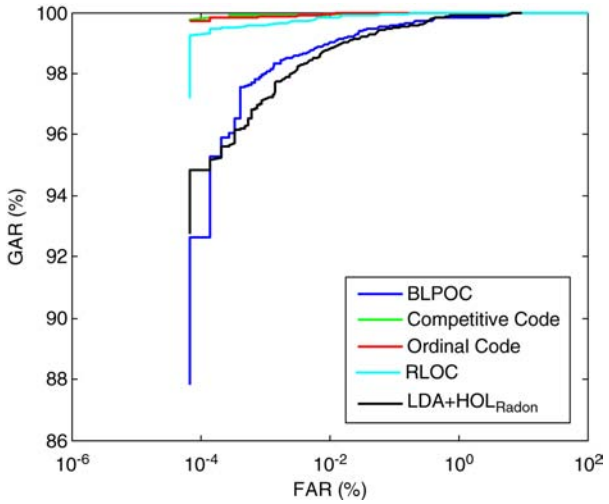

Fig. 12. ROC curves of methods BLPOC, competitive code, ordinal code, RLOC, and proposed method ($LDA + HOL_{Radon}$) on PolyU II database.

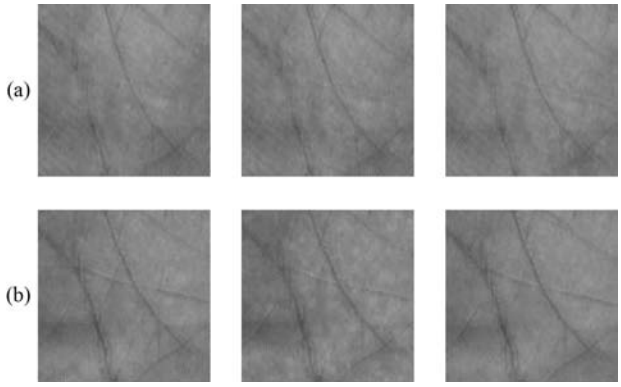

Fig. 13. Six palmprint ROI images from a same palm in PolyU II database. (a) Three images captured in the first session. (b) Three images captured in the second session.

From Table III, it can be seen that the identification performance of the proposed method is comparable to coding-based

TABLE V
RECOGNITION RATE (%) OF VECTOR-BASED METHODS ON DIFFERENT REPRESENTATIONS AND CORRESPONDING DIMENSION (IN THE INDENTIFICATION EXPERIMENTS ON POLYU M_B DATABASE)

	PCA	KPCA	LDA	KLDA	SRDA	KSRDA
OR	90.43 (200)	90.37 (230)	96.30 (70)	94.13 (380)	96.10 (360)	96.07 (360)
DR	97.60 (170)	97.77 (170)	97.97 (120)	96.70 (310)	97.37 (290)	97.43 (300)
HOG	98.73 (280)	98.77 (300)	99.17 (150)	99.13 (320)	99.00 (300)	99.37 (300)
$\text{HOL}_{\text{Gabor}}$	99.73 (370)	99.73 (370)	99.97 (330).	100 (330)	99.93 (340)	100 (290)
$\text{HOL}_{\text{Radon}}$	99.77 (350)	99.73 (370)	99.97 (200)	99.97 (350)	99.97 (340)	99.97 (290)

TABLE VI
RECOGNITION RATE (%) OF MATRIX OR TENSOR-BASED METHODS ON DIFFERENT REPRESENTATIONS AND CORRESPONDING DIMENSION (IN THE INDENTIFICATION EXPERIMENTS ON POLYU M_B DATABASE)

	2DPCA	2DLDA	TSA	CSA	MDA
OR	91.60 (128×18)	97.70 (128×12)	98.10 (13×13)	98.00 (9×9)	97.80 (11×11)
DR	97.87 (128×17)	98.67 (128×16)	98.83 (18×18)	98.43 (11×11)	99.00 (10×10)
2DHOG	98.50 (49×26)	98.90 (49×26)	98.37 (38×38)	96.60 (27×27)	98.87 (18×18)
$\text{2DHOL}_{\text{Gabor}}$	99.77 (49×40)	99.70 (49×27)	99.67 (37×37)	99.87 (24×24)	99.83 (38×38)
$\text{2DHOL}_{\text{Radon}}$	99.83 (49×38)	99.80 (49×35)	99.83 (33×33)	99.83 (15×15)	99.93 (33×33)

methods. However, in Table IV, the verification performance of the proposed method is worse than that of coding-based methods. This result demonstrates that the proposed method may be more suitable for identification.

C. Experimental Results on PolyU M_B Database

Fig. 13 depicts six palmprint ROI images of PolyU M_B database, which were captured from a same palm. The three images in first row [Fig. 13(a)] were captured in the first session while the images in second row [Fig. 13(b)] were captured in second session. In PolyU M_B database, the first three palmprints from the first session are used for training and the palmprints from the second session are adopted for test. So, the numbers of images for training and test are 1500 and 3000, respectively. In the experiments of HOL on PolyU M_B database, we adopted the same parameters determined in the experiments on PolyU II database.

Since BLPOC, RLOC, ordinal code, competitive code are four representative methods for palmprint recognition, we only select them to make performance comparison.

On PolyU M_B database, we firstly conduct identification experiments using different subspace learning methods on different palmprint representations. Tables V and VI list the recognition rates and corresponding dimensions of all subspace learning methods. Obviously, the recognition performances of HOL/2DHOL are also far better than that of OR, DR, and HOG/2DHOG representation. Specially, the recognition rate of proposed method is 100%, which is a very encouraging recognition result.

In order to make an identification performance comparison, we conduct identification experiments of methods RLOC, competitive code, ordinal code, and BLPOC. In these methods, we use the same parameter setting in the experiments of PolyU II database. Here, we select the recognition rate (100%) of $\text{KSRDA} + \text{HOL}_{\text{Gabor}}$ for performance comparison because it is the highest recognition rate achieved by the proposed method. The recognition rates of different methods are listed in Table VII. It can be seen that all methods achieved very high recognition rate, which is about 100%.

TABLE VII
RECOGNITION RATE OF DIFFERENT METHODS IN IDENTIFICATION EXPERIMENTS

Method	Recognition rate (%)
RLOC	100
Competitive code	100
Ordinal code	100
BLPOC	99.9
Proposed method	100

TABLE VIII
EER OF DIFFERENT METHODS IN VERIFICATION EXPERIMENTS CONDUCTED ON POLYU M_B DATABASE

	EER (%)
BLPOC	0.15
RLOC	0.03
Ordinal code	0.03
Competitive code	0
Proposed method	0.064

In verification experiments, five methods are tested, which are BLPOC, RLOC, ordinal code, competitive code, and the proposed method ($\text{LDA} + \text{HOL}_{\text{Radon}}$). Here, the dimension of LDA is set to 220. The EERs of five methods are listed in Table VIII. In PolyU M_B database, the EER of competitive code is 0, and the EER of proposed method is close to the methods of RLOC and ordinal code. In Fig. 14, we also illustrate the ROC curves of the methods BLPOC, ordinal code, RLOC, and the proposed method ($\text{LDA} + \text{HOL}_{\text{Radon}}$). As the EER of the method of competitive code is 0, its ROC curve is not depicted in Fig. 14. From Table VIII and Fig. 14, it can be seen that the performance of BLPOC is the worst.

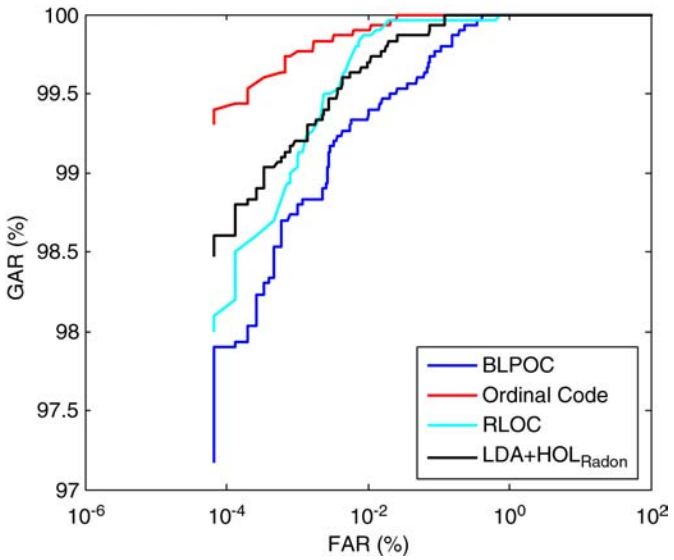

Fig. 14. ROC curves of methods BLPOC, ordinal code, RLOC, and the proposed method (LDA + HOL$_{Radon}$) on PolyU M_B database.

TABLE IX
TIME OF GENERATING DESCRIPTOR

Descriptor	Constructing time (ms)
HOG	12
HOL$_{Gabor}$	280
HOL$_{Radon}$	80

D. Time of Generating Descriptor

For real applications, the time of generating feature is an important issue. In this section, we report the time of generating descriptor. This paper is performed on a notebook PC with an Intel i5-2520 M CPU (2.50 GHz) and 4 GB RAM con-figured with Microsoft Windows 7 and MATLAB 2009 with image processing toolbox. The times of generating HOG, HOL$_{Gabor}$, and HOL$_{Radon}$ are 12, 280, and 80 ms, respectively, which are listed in Table IX. It could be seen that the speed of constructing HOL$_{Radon}$ is obviously faster than that of HOL$_{Gabor}$. In fact, we have not completely optimized the program codes, so it is possible for us to further reduce the computation time.

E. Discussions

As we have mentioned above, PolyU II is a challenging database because there are drastic changes of illumination between the images captured in different sessions. Those subspace learning methods using the proposed HOL desciptor can achieve much better recogniton rates than that of using OR. It could be concluded that the proposed HOL descriptor is robust to slight illumination changes. However, the verification performances of the proposed method are very different on these two databases. On the PolyU II database, the verification performance of the proposed method is obviously worse than that of three orientation-based methods. But, on the PolyU M_B database, the verification performance of the proposed method is close to three orientation-based methods. We know all images in PolyU M_B database are captured in a stable illumination condition. Therefore, we can say that subspace learning methods using the proposed HOL descriptor can achieve better verification performance in a stable illumination condition.

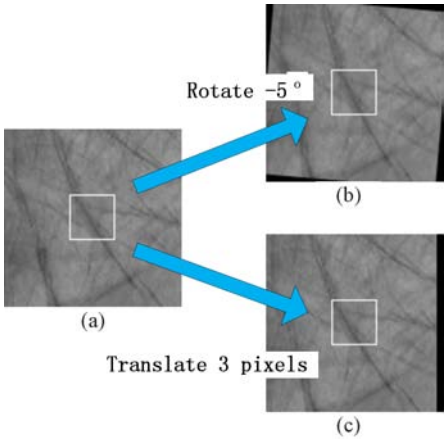

Fig. 15. *Blocks* within three images. (a) Original image. (b) Image after rotation. (c) Image after translation.

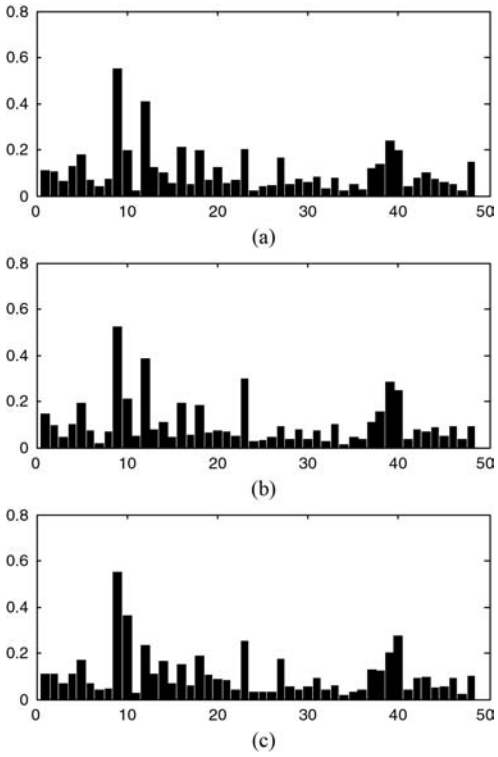

Fig. 16. Plotted histograms. (a) Plotted histogram of original *Block*. (b) Plotted histogram after rotation. (c) Plotted histogram after translation.

In this paper, we have mentioned that the proposed HOL has the robustness against small transformations because slight shifts and rotations make small histogram value changes. Here, an example is given. In HOL, the size of a *Cell* is 16×16, so the size of a *Block* containing 2×2 *Cells* is 32×32. In Fig. 15(a), a *Block* located in the center area is presented using a white square. In Fig. 15(b) and (c), two corresponding *Blocks* are illustrated after rotation (–5^o) and translation (three pixels), respectively. In Fig. 16, we plot

TABLE X
RECOGNITION RATES FOR DIFFERENT SHIFT VALUES

	0	1	2	3	4	5
PCA + HOL_{Radon}	99.69	99.53	99.33	98.63	96.51	92.13
PCA + OR	79.42	77.30	72.79	65.66	56.92	48.10
LDA + HOL_{Radon}	99.95	99.95	99.92	99.64	99.17	97.95
LDA + OR	94.15	92.60	88.38	81.72	72.82	60.96

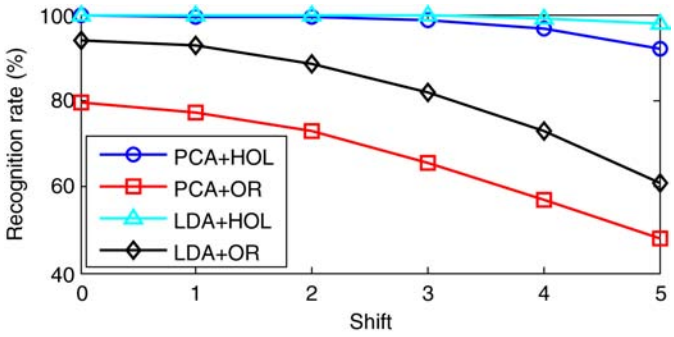

Fig. 17. Recognition rates for different shift values of m (m = 1, 2, 3,4, 5).

TABLE XI
RECOGNITION RATES FOR DIFFERENT ROTATION VALUES

	0°	−1°	−2°	−3°	−4°	−5°
PCA + HOL_{Radon}	99.69	99.56	99.33	98.84	98.84	95.19
PCA + OR	79.42	78.72	77.43	74.81	70.88	66.35
LDA + HOL_{Radon}	99.95	99.84	99.69	99.40	99.38	97.80
LDA + OR	94.15	93.53	92.80	91.30	88.58	84.75

the *Block* histograms (HOL_{Radon}) within Fig. 15(a)–(c) [see Fig. 16(a)–(c)], respectively. It can be seen that the changes of histogram values are small after image rotation and translation. Therefore, it is easy to understand why HOL descriptor can help subspace learning methods achieve promising recognition performance.

Here, we conduct some quantified identification experiments using PCA and LDA on PolyU II database to further show that the proposed HOL descriptor is robust to small transformations. In the first experiment, the training set (1158 images) is unchanged, but all images (3863 images) in probe set shift m (m = 1, 2, 3, 4, 5) pixels toward the left [see Fig. 15(c)]. The recognition rates of PCA and LDA on HOL_{radon} and OR are listed in Table X. In addition, corresponding results are depicted in Fig. 17. In the second experiment, the training set (1158 images) is also unchanged, but all images (3863 images) in probe set rotate k (k = –1°, –2°, –3°, –4°, –5°) degree [see Fig. 15(b)]. The recognition rates of PCA and LDA on HOL_{radon} and OR are listed in Table XI. In, addition, corresponding results are depicted in Fig. 18. These results clearly show that small transformations have limited effect for the performance of the methods of PCA + HOL_{radon} and LDA + HOL_{radon}, but will drastically reduce the recognition rates of PCA + OR and LDA + OR.

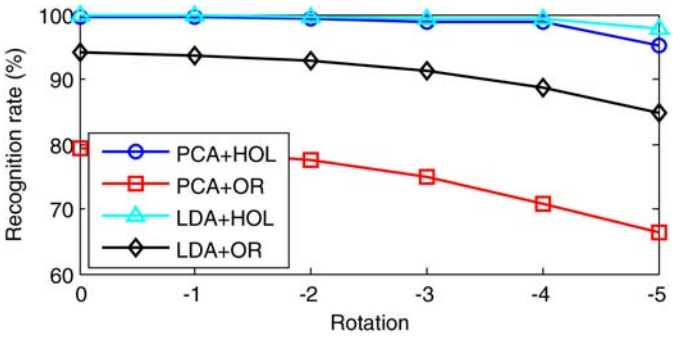

Fig. 18. Recognition rates for different rotation values of k (k = –1°, –2°, –3°, –4°, –5°).

IV. CONCLUSION

This paper investigated how to improve the recognition performance of subspace learning methods for palmprint recognition. To do this, we proposed a new descriptor of palmprint named HOL, which is robust to slight illumination, translation, and rotation variances, and has better discriminative power than OR, DR, and GWR. As a result, even some simple subspace learning methods such as PCA and LDA can achieve very promising recognition performances on PolyU II and PolyU M_B databases. In our future work, we will adopt other strategies to further improve the discriminative power of HOL descriptor.

ACKNOWLEDGMENT

The authors would like to thank the Biometric Research Center at The Hong Kong Polytechnic University for providing the PolyU Palmprint Databases.

REFERENCES

[1] D. Zhang, A. Kong, J. You, and M. Wong, "Online palmprint identification," *IEEE Trans. Pattern Anal. Mach. Intell.*, vol. 25, no. 9, pp. 1041–1050, Sep. 2003.
[2] A. Kong, D. Zhang, and M. Kamel, "A survey of pamprint recognition," *Pattern Recognit.*, vol. 42, no. 7, pp. 1408–1418, 2009.
[3] D. S. Huang, W. Jia, and D. Zhang, "Palmprint verification based on principal lines," *Pattern Recognit.*, vol. 41, no. 4, pp. 1316–1328, 2008.
[4] X. Q. Wu, D. Zhang, and K.Q. Wang, "Palm line extraction and matching for personal authentication," *IEEE Trans. Syst., Man, Cybern. A, Syst. Humans*, vol. 36, no. 5, pp. 978–987, Sep. 2006.
[5] Z. N. Sun, T. N. Tan, Y. H. Wang, and S. Z. Li, "Ordinal palmprint representation for personal identification," in *Proc. CVPR*, 2005, pp. 279–284.
[6] W. Jia, D.S. Huang, and D. Zhang, "Palmprint verification based on robust line orientation code," *Pattern Recognit.*, vol. 41, no. 5, pp. 1504–1513, 2008.
[7] A. Kong and D. Zhang, "Competitive coding scheme for palmprint verification," in *Proc. 17th ICPR*, 2004, vol. 1, pp. 520–523.
[8] F. Yue, W.M. Zuo, and D. Zhang, "FCM-based orientation selection for competitive code-based palmprint recogniton," *Pattern Recognit.*, vol. 42, no. 11, pp. 2841–2849, 2009.
[9] Z. H. Guo, D. Zhang, L. Zhang, and W. M. Zuo, "Palmprint verification using binary orientation co-occurrence vector," *Pattern Recognit. Lett.*, vol. 30, no. 13, pp. 1219–1227, 2009.
[10] P. Hennings-Yeomans, B. Kumar, and M. Savvides, "Palmprint classification using multiple advanced correlation filters and palm-specific segmentation," *IEEE Trans. Inform. Forensics Security*, vol. 2, no. 3, pp. 613–622, Sep. 2007.

[11] K. Ito, T. Aoki, and H. Nakajima, "A palmprint recognition algorithm using phase-only correlation," *IEICE Trans. Fundam.*, vol. e91-a, no. 4, pp. 1023–1030, 2008.

[12] W. Li, D. Zhang, G. Lu, and N. Luo, "A novel 3-D palmprint acquisition system," *IEEE Trans. Syst., Man, Cybern. A, Syst. Humans*, vol. 42, no. 2, pp. 443–452, Mar. 2012.

[13] P. Belhumeur, J. Hespanha, and D. Kriegman, "Eigenfaces vs. fisherfaces: Recognition using class specific linear projection," *IEEE Trans. Pattern Anal. Mach. Intell.*, vol. 19, no. 7, pp. 711–720, Jul. 1997.

[14] J. Yang, A. Frangi, J. Yang, D. Zhang, and J. Zhong, "KPCA plus LDA: A complete kernel fisher discriminant framework for feature extraction and recognition," *IEEE Trans. Pattern Anal. Mach. Intell.*, vol. 27, no. 2, pp. 230–244, Feb. 2005.

[15] J. Yang, D. Zhang, A. Frangi, and J. Yang, "Two-dimensional PCA: A new approach to appearance-based face representation and recognition," *IEEE Trans. Pattern Anal. Mach. Intell.*, vol. 26, no. 1, pp. 131–137, Jan. 2004.

[16] M. Li and B. Yuan, "2D-LDA: A novel statistical linear discriminant analysis for image matrix," *Pattern Recognit. Lett.*, vol. 26, no. 5, pp. 527–532, 2005.

[17] D. Cai, X. He, and J. Han, "Subspace learning based on tensor analysis," Comput. Sci. Dept., UIUC, Tech. Rep. UIUCDCS-R-2005–2572, May 2005.

[18] D. Xu, S. Yan, L. Zhang, S. Lin, H. Zhang, and T. Huang, "Reconstruction and recognition of tensor-based objects with concurrent subspaces analysis," *IEEE Trans. Circuits Syst. Video Technol.*, vol. 18, no. 1, pp. 36–47, Jan. 2008.

[19] S. C. Yan, D. Xu, Q. Yang, L. Zhang, X. Tang, and H. J. Zhang, "Multilinear discriminant analysis for face recognition," *IEEE Trans. Image Process.*, vol. 16, no. 1, pp. 212–219, Jan. 2007.

[20] G. M. Lu, D. Zhang, and K. Q. Wang, "Palmprint recognition using eigenpalms features," *Pattern Recognit. Lett.*, vol. 24, nos. 9–10, pp. 1463–1467, 2003.

[21] X. Q. Wu, D. Zhang, and K. Q. Wang, "Fisherpalms based palmprint recognition," *Pattern Recognit. Lett.*, vol. 24, no. 15, pp. 2829–2838, 2003.

[22] T. Connie, A. T. B. Jin, M. G. K. On, and D. N. C. Ling, "An automated palmprint recognition system," *Image Vis. Comput.*, vol. 23, no. 5, pp. 501–515, 2005.

[23] D. Hu, G. Feng, and Z. Zhou, "Two-dimensional locality preserving projecting (2DLPP) with its application to palmprint recognition," *Pattern Recognit.*, vol. 40, no. 3, pp. 339–342, 2007.

[24] J. Yang, D. Zhang, J. Y. Yang, and B. Niu, "Globally maximizing, locally minimizing: Unsupervised discriminant projection with applications to face and palm biometrics," *IEEE Trans. Pattern Anal. Mach. Intell.*, vol. 29, no. 4, pp. 650–664, Apr. 2007.

[25] W. M. Zuo, H. Z. Zhang, D. Zhang, and K. Q. Wang, "Post-processed LDA for face and palmprint recognition: What is the rationale," *Signal Process.*, vol. 90, no. 8, pp. 2344–2352, 2010.

[26] M. Ekinci and M. Aykut, "Gabor-based kernel PCA for palmprint recognition," *Electron. Lett.*, vol. 43, no. 20, pp. 1077–1079, 2007.

[27] X. Pan and Q. Q. Ruan, "Palmprint recognition using Gabor feature-based $(2D)^2$PCA," *Neurocomputing*, vol. 71, no. 13–15, pp. 3032–3036, 2008.

[28] X. Pan and Q. Q. Ruan, "Palmprint recognition with improved two-dimensional locality preserving projections," *Image Vis. Comput.*, vol. 26, no. 9, pp. 1261–1268, 2008.

[29] R. Chu, Z. Lei, Y. Han, R. He, and S. Z. Li, "Learning Gabor magnitude features for palmprint recognition," in *Proc. ACCV—Part II*, LNCS 4844. 2007, pp. 22–31.

[30] W. Jia, D.S. Huang, D. Tao, and D. Zhang, "Palmprint identification based on directional represention," in *Proc. IEEE Int. Conf. SMC*, 2008, pp. 1562–1567.

[31] D. Lowe, "Distinctive image feature from scale-invariant key-point," *Int. J. Comput. Vis.,* vol. 60, no. 2, pp. 91–110, 2004.

[32] N. Dalal and B. Triggs, "Histograms of oriented gradients for human detection," in *Proc. 9th Eur. Conf. CV*, San Diego, CA, USA, Jun. 2005.

[33] Y. F. Han, T. N. Tan, and Z. N. Sun, "Palmprint recognition based on directional features and graph matching," in *Proc. ICB*, 2007, pp. 1164–1173.

[34] S. F. Xie, S. G. Shan, X. L. Chen, J. Chen, "Fusing local patterns of Gabor magnitude and phase for face recognition," *IEEE Trans. Image Process.*, vol. 19, no. 5, pp. 1349–1361, May 2010.

[35] W. C. Zhang, S. G. Shan, W. Gao *et al*., "Local gabor binary pattern histogram sequence (LGBPHS): A novel non-statistical model for face representation and recognition," in *Proc. 10th IEEE Int. Conf. Comput. Vis.*, vols. 1–2. 2005, pp. 786–791.

[36] D. Zhang, Z. H. Guo, G. M. Lu, L. Zhang, and W. M. Zuo, "An online system of multispectral palmprint verification," *IEEE Trans. Instrum. Meas.*, vol. 59, no. 2, pp. 480–490, Feb. 2010.

[37] D. Cai, X. F. He, and J. W. Han, "SRDA: An efficient algorithm for large-scale discriminant analysis," *IEEE Trans. Knowl. Data Eng.*, vol. 20, no. 1, pp. 1–12, Jan. 2008.

[38] B. Kumar, V. Savvides, C. Xie, "Correlation pattern recognition for face recognition," *Proc. IEEE*, vol. 94, no. 11, pp. 1963–1976, Nov. 2006.